

Contents lists available at [SciVerse ScienceDirect](http://SciVerse.ScienceDirect.com)

## Physics Letters B

[www.elsevier.com/locate/physletb](http://www.elsevier.com/locate/physletb)Supersymmetric contribution to  $B \rightarrow \rho K$  and  $B \rightarrow \pi K^*$  decays in SCETGaber Faisal<sup>a,b,\*</sup>, David Delepine<sup>c</sup>, M. Shalaby<sup>d</sup><sup>a</sup> Department of Physics and Center for Mathematics and Theoretical Physics, National Central University, Chung-li, 32054, Taiwan<sup>b</sup> Egyptian Center for Theoretical Physics, Modern University for Information and Technology, Cairo, Egypt<sup>c</sup> Departamento de Física, DCl, Campus León, Universidad de Guanajuato, C.P. 37150, León, Guanajuato, Mexico<sup>d</sup> Ain Shams University, Faculty of Science, Cairo 11566, Egypt

## ARTICLE INFO

## Article history:

Received 15 February 2011

Received in revised form 4 October 2011

Accepted 18 October 2011

Available online 20 October 2011

Editor: T. Yanagida

## ABSTRACT

We analyze the supersymmetric contributions to the direct CP asymmetries of the decays  $B \rightarrow \pi K^*$  and  $B \rightarrow \rho K$  within Soft Collinear Effective Theory. We extend the Standard Model analysis of these asymmetries to include the next leading order QCD corrections. We find that, even with QCD correction, the Standard Model predictions cannot accommodate the direct CP asymmetries in these decay modes. Using Mass Insertion Approximation (MIA), we show that non-minimal flavor SUSY contributions mediated by gluino exchange can enhance the CP asymmetries significantly and thus can accommodate the experimental results.

© 2011 Elsevier B.V. Open access under [CC BY license](http://creativecommons.org/licenses/by/3.0/).

## 1. Introduction

In the standard model (SM), Charge conjugation Parity (CP) violation and flavor transition arise from the complex Yukawa couplings in the Cabibbo Kobayashi Maskawa (CKM) matrix. The effect of this phase has been first observed in kaon system and confirmed in  $B$  decays. However, the expected CP asymmetries in some decay channels for  $B$  meson are in contradiction with the experimental measurements carried by Babar and Belle  $B$ -factories and proton antiproton collider as Tevatron, with its experiments CDF and D0. The largest discrepancy has been observed in the decay  $B \rightarrow K\pi$  where the world averages for the CP asymmetries of  $B^0 \rightarrow K^\pm \pi^\mp$  and  $B^\pm \rightarrow K^\pm \pi^0$  are given by [1]:

$$\mathcal{A}_{\text{CP}}(B^0 \rightarrow K^\pm \pi^\mp) = -0.098 \pm 0.012, \quad (1)$$

$$\mathcal{A}_{\text{CP}}(B^\pm \rightarrow K^\pm \pi^0) = 0.050 \pm 0.025, \quad (2)$$

which implies that

$$\begin{aligned} \Delta \mathcal{A}_{\text{CP}} &= \mathcal{A}_{\text{CP}}(B^\pm \rightarrow K^\pm \pi^0) - \mathcal{A}_{\text{CP}}(B^0 \rightarrow K^\pm \pi^\mp) \\ &= 0.14 \pm 0.029. \end{aligned} \quad (3)$$

In the SM and using QCD factorization approach, the results of the above two asymmetries read [2]:

$$\mathcal{A}_{\text{CP}}(B^\pm \rightarrow K^\pm \pi^0) = (7.1^{+1.7+2.0+0.8+9.0}_{-1.8-2.0-0.6-9.7})\%, \quad (4)$$

\* Corresponding author at: Department of Physics and Center for Mathematics and Theoretical Physics, National Central University, Chung-li, 32054, Taiwan.

E-mail address: [gfaisel@cc.ncu.edu.tw](mailto:gfaisel@cc.ncu.edu.tw) (G. Faisal).

$$\mathcal{A}_{\text{CP}}(B^0 \rightarrow K^\pm \pi^\mp) = (4.5^{+1.1+2.2+0.5+8.7}_{-1.1-2.5-0.6-9.5})\%, \quad (5)$$

where the first error corresponds to uncertainties on the CKM parameters and the other three errors correspond to variation of various hadronic parameters. These results imply that  $\Delta \mathcal{A}_{\text{CP}}^{\text{QCD}} = 0.025 \pm 0.015$ , which differs from the experimental value by  $3.5\sigma$  and thus motivate exploring new physics beyond SM.

The decay modes  $B \rightarrow \pi K^*$  and  $B \rightarrow \rho K$  are generated at the quark level in the same way as  $B \rightarrow K\pi$  and hence it is interesting to explore hints of New Physics (NP) in these decays. These decay modes are studied within SM in framework of QCDF [2], PQCD [3,4,6,5] and Soft Collinear Effective Theory (SCET) [7]. A detailed comparison between the results for the branching ratios and CP asymmetries in these different factorizations methods can be found in Ref. [7]. The comparison showed that PQCD results for most  $B \rightarrow \pi K^*$  and  $B \rightarrow \rho K$  channels are much larger than SCET results. On the other hand the QCDF results are small and comparable with SCET results but with a relative minus sign. Moreover, in SCET, the direct CP asymmetries of  $B^- \rightarrow \pi^- \bar{K}^{*0}$  and  $B^- \rightarrow \rho^- \bar{K}^0$  are zero while the CP asymmetries in other channels are small. Recently, in Ref. [8] fits to  $B \rightarrow \pi K^*$  and  $B \rightarrow \rho K$  decays are performed where data can be accommodated within the standard model due principally to the large experimental uncertainties, particularly in the CP-violating asymmetries.

One of the four large experiments operating at the Large Hadron Collider (LHC) is LHCb. The main task of the LHCb is to measure precisely the CP asymmetries in  $B$  meson decays. These measurements are so important to test the different mechanisms proposed by many models beyond SM to explain the matter–antimatter asymmetry. This test can be regarded as an indirect search for physics beyond SM.

Supersymmetry (SUSY) is one of the most interesting candidates for physics beyond the standard model as it naturally solves the hierarchy problem. In addition, SUSY has new sources for CP violation which can account for the baryon number asymmetry and affect other CP violating observables in the  $B$  and  $K$  decays. The effects of these phases on the CP asymmetries in semi-leptonic  $\tau$  decays has been studied in Refs. [11,10,9].

In this Letter, we analyze the SUSY contributions to the CP asymmetries of the  $B \rightarrow \pi K^*$  and  $B \rightarrow \rho K$  decays in the framework of SCET [12–15]. SCET is an effective field theory describing the dynamics of highly energetic particles moving close to the light-cone interacting with a background field of soft quanta [16]. It provides a systematic and rigorous way to deal with the decays of the heavy hadrons that involve different energy scales. The scaling of fields and momenta in SCET depends on a small parameter  $\lambda$ . Generally  $\lambda$  is defined as the ratio of the smallest and the largest energy scales in the given process. Then, the SCET Lagrangian and effective Hamiltonian are expanded in terms of  $\lambda$  that help to reduce the complexity of the calculations. In addition, the factorization formula provided by SCET is perturbative to all powers in  $\alpha_s$  expansion.

This Letter is organized as follows. In Section 2, we briefly review the decay amplitude for  $B \rightarrow M_1 M_2$  within SCET framework. Accordingly, we analyze the CP asymmetries and branching ratios for  $B \rightarrow \pi K^*$  and  $B \rightarrow \rho K$  within SM in Section 3. In Section 4, we discuss the SUSY contributions to the CP asymmetries of the  $B \rightarrow \pi K^*$  and  $B \rightarrow \rho K$  decays. We give our conclusion in Section 5.

## 2. $B \rightarrow M_1 M_2$ in SCET

The amplitude of  $B \rightarrow M_1 M_2$  where  $M_1$  and  $M_2$  are light mesons in SCET can be written as follows

$$\mathcal{A}_{B \rightarrow M_1 M_2}^{\text{SCET}} = \mathcal{A}_{B \rightarrow M_1 M_2}^{\text{LO}} + \mathcal{A}_{B \rightarrow M_1 M_2}^{\text{X}} + \mathcal{A}_{B \rightarrow M_1 M_2}^{\text{ann}} + \mathcal{A}_{B \rightarrow M_1 M_2}^{\text{c.c.}} \quad (6)$$

Here  $\mathcal{A}_{B \rightarrow M_1 M_2}^{\text{LO}}$  denotes the leading order amplitude in the expansion  $1/m_b$ ,  $\mathcal{A}_{B \rightarrow M_1 M_2}^{\text{X}}$  denotes the chirally enhanced penguin amplitude,  $\mathcal{A}_{B \rightarrow M_1 M_2}^{\text{ann}}$  denotes the annihilation amplitude and  $\mathcal{A}_{B \rightarrow M_1 M_2}^{\text{c.c.}}$  denotes the long distance charm penguin contributions. In the following we give a brief account for each amplitude.

### 2.1. Leading order amplitude

At leading power in  $(1/m_b)$  expansion, the full QCD effective weak Hamiltonian of the  $\Delta_B = 1$  decays is matched into the corresponding weak Hamiltonian in SCET<sub>I</sub> by integrating out the hard scale  $m_b$ . Then, the SCET<sub>I</sub> weak Hamiltonian is matched into the weak Hamiltonian SCET<sub>II</sub> by integrating out the hard collinear modes with  $p^2 \sim \Lambda m_b$  and the amplitude of the  $\Delta_B = 1$  decays at leading order in  $\alpha_s$  expansion can be obtained via [17]:

$$\begin{aligned} \mathcal{A}_{B \rightarrow M_1 M_2}^{\text{LO}} &= -i \langle M_1 M_2 | H_W^{\text{SCET}_{II}} | \bar{B} \rangle \\ &= \frac{G_F m_B^2}{\sqrt{2}} \left( f_{M_1} \left[ \int_0^1 du dz T_{M_1 J}(u, z) \zeta_J^{BM_2}(z) \phi_{M_1}(u) \right. \right. \\ &\quad \left. \left. + \zeta^{BM_2} \int_0^1 du T_{M_1 \zeta}(u) \phi_{M_1}(u) \right] + (M_1 \leftrightarrow M_2) \right). \end{aligned} \quad (7)$$

At leading order in  $\alpha_s$  expansion, the parameters  $\zeta^{B(M_1, M_2)}$ ,  $\zeta_J^{B(M_1, M_2)}$  are treated as hadronic parameters and can be determined through the  $\chi^2$  fit method using the nonleptonic decay experimental data of the branching fractions and CP asymmetries. At first order in  $\alpha_s$  expansion,  $\zeta_J^{BM}(z)$  can be written as a polynomial in  $z$  as follows [18]

$$\zeta_J^{BM}(z) = 2z \zeta_J^{BM} - A_1^{BM} (4z - 6z^2) + \frac{5}{6} A_2^{BM} (z - 6z^2 + 6z^3), \quad (8)$$

where again  $\zeta_J^{BM}$  are treated as hadronic parameters which are determined through the fit to the nonleptonic decay data. The hard kernels  $T_{(M_1, M_2) \zeta}$  and  $T_{(M_1, M_2) J}$  are expressed in terms of  $c_i^{(f)}$  and  $b_i^{(f)}$  which are functions of the Wilson coefficients as follows [18]

$$\begin{aligned} T_{1\zeta}(u) &= C_{u_L}^{BM_2} C_{f_L u}^{M_1} c_1^{(f)}(u) + C_{f_L}^{BM_2} C_{u_L}^{M_1} c_2^{(f)}(u) \\ &\quad + C_{f_L}^{BM_2} C_{u_R}^{M_1} c_3^{(f)}(u) + C_{q_L}^{BM_2} C_{f_L q}^{M_1} c_4^{(f)}(u), \\ T_{1J}(u, z) &= C_{u_L}^{BM_2} C_{f_L u}^{M_1} b_1^{(f)}(u, z) + C_{f_L}^{BM_2} C_{u_L}^{M_1} b_2^{(f)}(u, z) \\ &\quad + C_{f_L}^{BM_2} C_{u_R}^{M_1} b_3^{(f)}(u, z) + C_{q_L}^{BM_2} C_{f_L q}^{M_1} b_4^{(f)}(u, z), \end{aligned} \quad (9)$$

here  $f$  stands for  $d$  or  $s$  and  $C_i^{BM}$  and  $C_i^M$  are Clebsch–Gordan coefficients that depend on the flavor content of the final states. For instance, we have  $C_{u_L}^{B^0 \pi^+} = +1$ ,  $C_{d_L}^{\pi^-} = +1$ ,  $C_{d_R}^{\pi^-} = -1$ ,  $C_{u_L}^{B^0 \rho^+} = +1$ , and  $C_{d_L}^{\rho^-} = C_{d_R}^{\rho^-} = +1$ ,  $C_{d_L}^{B^- \pi^-} = +1$  and  $C_{u_R}^{\pi^0} = -\frac{1}{\sqrt{2}}$  and  $c_i^{(f)}$  and  $b_i^{(f)}$  are given by [19]

$$\begin{aligned} c_{1,2}^{(f)} &= \lambda_u^{(f)} \left[ C_{1,2} + \frac{1}{N} C_{2,1} \right] - \lambda_t^{(f)} \frac{3}{2} \left[ \frac{1}{N} C_{9,10} + C_{10,9} \right] + \Delta c_{1,2}^{(f)}, \\ c_3^{(f)} &= -\frac{3}{2} \lambda_t^{(f)} \left[ C_7 + \frac{1}{N} C_8 \right] + \Delta c_3^{(f)}, \\ c_4(f) &= -\lambda_t^{(f)} \left[ \frac{1}{N} C_3 + C_4 - \frac{1}{2N} C_9 - \frac{1}{2} C_{10} \right] + \Delta c_4^{(f)}, \end{aligned} \quad (10)$$

and

$$\begin{aligned} b_{1,2}^{(f)} &= \lambda_u^{(f)} \left[ C_{1,2} + \frac{1}{N} \left( 1 - \frac{m_b}{\omega_3} \right) C_{2,1} \right] \\ &\quad - \lambda_t^{(f)} \frac{3}{2} \left[ C_{10,9} + \frac{1}{N} \left( 1 - \frac{m_b}{\omega_3} \right) C_{9,10} \right] + \Delta b_{1,2}^{(f)}, \\ b_3^{(f)} &= -\lambda_t^{(f)} \frac{3}{2} \left[ C_7 + \left( 1 - \frac{m_b}{\omega_2} \right) \frac{1}{N} C_8 \right] + \Delta b_3^{(f)}, \\ b_4^{(f)} &= -\lambda_t^{(f)} \left[ C_4 + \frac{1}{N} \left( 1 - \frac{m_b}{\omega_3} \right) C_3 \right] \\ &\quad + \lambda_t^{(f)} \frac{1}{2} \left[ C_{10} + \frac{1}{N} \left( 1 - \frac{m_b}{\omega_3} \right) C_9 \right] + \Delta b_4^{(f)}, \end{aligned} \quad (11)$$

where  $\omega_2 = m_b u$  and  $\omega_3 = -m_b \bar{u}$ .  $u$  and  $\bar{u} = 1 - u$  are momentum fractions for the quark and antiquark  $\bar{n}$  collinear fields. The  $\Delta c_i^{(f)}$  and  $\Delta b_i^{(f)}$  denote terms depending on  $\alpha_s$  generated by matching from  $H_W$ . The  $\mathcal{O}(\alpha_s)$  contribution to  $\Delta c_i^{(f)}$  has been calculated in Refs. [21,20,15] and later in Ref. [18] while the  $\mathcal{O}(\alpha_s)$  contribution to  $\Delta b_i^{(f)}$  has been calculated in Refs. [22,23,18].

### 2.2. Chirally enhanced penguins amplitude

Corrections of order  $\alpha_s(\mu_h)(\mu_M \Lambda/m_b^2)$  where  $\mu_M$  is the chiral scale parameter generate the so called Chirally enhanced penguins

amplitude  $\mathcal{A}_{B \rightarrow M_1 M_2}^X$  [18].  $\mu_M$  for kaons and pions can be of order (2 GeV) and therefore chirally enhanced terms can compete with the order  $\alpha_s(\mu_h)(\Lambda/m_b)$  terms. The chirally enhanced amplitude for  $B \rightarrow M_1 M_2$  decays is given by [18]

$$\begin{aligned} & \mathcal{A}^X(\bar{B} \rightarrow M_1 M_2) \\ &= \frac{G_F m_B^2}{\sqrt{2}} \left\{ -\frac{\mu_{M_1} f_{M_1}}{3m_B} \zeta^{BM_2} \int_0^1 du R_1(u) \phi_{pp}^{M_1}(u) + (1 \leftrightarrow 2) \right. \\ & \quad - \frac{\mu_{M_1} f_{M_1}}{3m_B} \int_0^1 du dz R_1^J(u, z) \zeta_J^{BM_2}(z) \phi_{pp}^{M_1}(u) + (1 \leftrightarrow 2) \\ & \quad \left. - \frac{\mu_{M_2} f_{M_1}}{6m_B} \int_0^1 du dz R_1^X(u, z) \zeta_\chi^{BM_2}(z) \phi^{M_1}(u) + (1 \leftrightarrow 2) \right\}. \end{aligned} \quad (12)$$

The factors  $\mu_M$  are generated by pseudoscalars and so they vanish for vector mesons [18]. The pseudoscalar light cone amplitude  $\phi_{pp}^M(u)$  is defined as [25,24]

$$\begin{aligned} \phi_{pp}^P(u) &= 3u \left[ \phi_p^P(u) + \phi_\sigma^{P'}(u)/6 \right. \\ & \quad \left. + 2f_{3P}/(f_P \mu_P) \int dy' / y' \phi_{3P}(y - y', y) \right]. \end{aligned} \quad (13)$$

$\phi_{pp}^M$  are commonly expressed in terms of the first few terms in the Gegenbauer series

$$\phi_{pp}^M(x) = 6x(1-x) \left\{ 1 + a_{1pp}^M(6x-3) + 6a_{2pp}^M(1-5x+5x^2) \right\}. \quad (14)$$

As before, following the same procedure for treating  $\zeta_J^{BM}(z)$  we take  $\zeta_\chi^{BM}(z)$  as [18]

$$\zeta_\chi^{BM}(z) = 2z\zeta_\chi^{BM} - A_{\chi 1}^{BM}(4z-6z^2) + \frac{5}{6}A_{\chi 2}^{BM}(z-6z^2+6z^3). \quad (15)$$

The hard kernels  $R_K, R_\pi, R_K^J, R_\pi^J, R_K^X$  and  $R_\pi^X$  can be expressed in terms of Clebsch-Gordan coefficients for the different final states as [18]

$$\begin{aligned} R_1(u) &= C_{q_R}^{BM_2} C_{f_l q}^{M_1} \left[ c_{1(qf q)}^X + \frac{3}{2} e_q c_{2(qf q)}^X \right], \\ R_1^J(u, z) &= C_{q_R}^{BM_2} C_{f_l q}^{M_1} \left[ b_{3(qf q)}^X + \frac{3}{2} e_q b_{4(qf q)}^X \right], \\ R_1^X(u, z) &= C_{q_L}^{BM_2} C_{f_l q}^{M_1} b_{1(qf q)}^X + C_{u_L}^{BM_2} C_{f_l u}^{M_1} b_{1(uf u)}^X \\ & \quad + C_{f_l}^{BM_2} C_{u_L u}^{M_1} b_{1(fuu)}^X + C_{f_l}^{BM_2} C_{u_R u}^{M_1} b_{2(fuu)}^X. \end{aligned} \quad (16)$$

Summation over  $q = u, d, s$  is implicit and  $c_i^X$  and  $b_i^X$  are expressed in terms of the short distance Wilson coefficients as [18]

$$\begin{aligned} c_{1(qf q)}^X &= \lambda_t^{(f)} \left( C_6 + \frac{C_5}{N_c} \right) \frac{1}{u\bar{u}} + \Delta c_{1(qf q)}^X, \\ c_{2(qf q)}^X &= \lambda_t^{(f)} \left( C_8 + \frac{C_7}{N_c} \right) \frac{1}{u\bar{u}} + \Delta c_{2(qf q)}^X, \\ b_{1(qf q)}^X &= 2\lambda_t^{(f)} \left[ \frac{(1+uz)}{uz} \left( \frac{C_3}{N_c} - \frac{C_9}{2N_c} \right) + C_4 - \frac{C_{10}}{2} \right] + \Delta b_{1(qf q)}^X, \end{aligned}$$

$$\begin{aligned} b_{2(fuu)}^X &= 3\lambda_t^{(f)} \left[ C_7 + \frac{C_8}{N_c} - \frac{1}{uz} \frac{C_8}{N_c} \right] + \Delta b_{2(fuu)}^X, \\ b_{3(qf q)}^X &= \lambda_t^{(f)} \frac{1}{u\bar{u}} \left( C_6 + \frac{C_5}{N_c} \right) + \Delta b_{3(qf q)}^X, \\ b_{4(qf q)}^X &= \lambda_t^{(f)} \frac{1}{u\bar{u}} \left( C_8 + \frac{C_7}{N_c} \right) + \Delta b_{4(qf q)}^X, \\ b_{1(ufu)}^X &= \frac{2(1+uz)}{uz} \left( -\frac{C_2}{N_c} \lambda_u^{(f)} + \frac{3C_9}{2N_c} \lambda_t^{(f)} \right) \\ & \quad - (2C_1 \lambda_u^{(f)} - 3C_{10} \lambda_t^{(f)}) + \Delta b_{1(ufu)}^X, \\ b_{1(fuu)}^X &= \frac{2(1+uz)}{uz} \left( -\lambda_u^{(f)} \frac{C_1}{N_c} + \lambda_t^{(f)} \frac{3C_{10}}{2N_c} \right) \\ & \quad - (2C_2 \lambda_u^{(f)} - 3C_9 \lambda_t^{(f)}) + \Delta b_{1(fuu)}^X. \end{aligned} \quad (17)$$

The  $\Delta c_i^X$  and  $\Delta b_i^X$  terms denote perturbative corrections that can be found in Ref. [18].

### 2.3. Annihilation amplitudes

Annihilation amplitudes  $\mathcal{A}_{B \rightarrow M_1 M_2}^{ann}$  have been studied in PQCD and QCD factorization in Refs. [26–29]. Within SCET, the annihilation contribution becomes factorizable and real at leading order,  $\mathcal{O}(\alpha_s(m_b)\Lambda/m_b)$  [30]. In our numerical calculation, we do not include the contributions from penguin annihilation as their size is small and contains large uncertainty compared to the other contributions [24,18].

### 2.4. Long distance charm penguin amplitude

The long distance charm penguin amplitude  $\mathcal{A}_{B \rightarrow M_1 M_2}^{c.c}$  is given as follows

$$\mathcal{A}_{B \rightarrow M_1 M_2}^{c.c} = |\mathcal{A}_{B \rightarrow M_1 M_2}^{c.c}| e^{i\delta_{cc}} \quad (18)$$

where  $\delta_{cc}$  is the strong phase of the charm penguin. The modulus and the phase of the charm penguin are fixed through the fitting with nonleptonic decays in a similar way to the hadronic parameters  $\zeta^{B(M_1, M_2)}$ ,  $\zeta_J^{B(M_1, M_2)}$ .

### 3. SM contribution to the CP asymmetries and branching ratios of $B \rightarrow \pi K^*$ and $B \rightarrow \rho K$ decays

In this section, we analyze the SM contribution to the CP asymmetries and the branching ratios for  $B \rightarrow \pi K^*$  and  $B \rightarrow \rho K$  decays. We follow Ref. [18] and work in the next leading order of  $\alpha_s$  expansion. We take  $\alpha_s(m_Z) = 0.118$ ,  $m_t = 170.9$  GeV,  $m_b = 4.7$  GeV and the Wilson coefficients  $C_i$  can be found in Ref. [31]. For the other hadronic parameters, we use the same input values given in Ref. [18]. For the charm penguin parameters we use the values listed in Ref. [7].

The decay modes  $B \rightarrow \pi K^*$  and  $B \rightarrow \rho K$  are generated at the quark level via  $b \rightarrow s$  transition and thus we can decompose their amplitudes  $\mathcal{A}$  according to the unitarity of the CKM matrix as

$$\mathcal{A} = \lambda_u^s (\mathcal{A}_u^{\text{tree}} + \mathcal{A}_u^{\text{QCD}} + \mathcal{A}_u^{\text{EW}}) + \lambda_c^s (\mathcal{A}_c^{\text{cc}} + \mathcal{A}_c^{\text{non-cc}}). \quad (19)$$

Here  $\lambda_p^s = V_{pb} V_{ps}^*$  with  $p = u, c$  and  $\mathcal{A}_u^{\text{tree}}, \mathcal{A}_u^{\text{QCD}}, \mathcal{A}_u^{\text{EW}}$  refer to tree, QCD penguin and Electroweak penguins amplitudes respectively.  $\mathcal{A}_c^{\text{cc}}$  refers to long distance charming penguin and  $\mathcal{A}_c^{\text{non-cc}}$  refers to contributions from other QCD and Electroweak penguins. It should be noted here that, the different amplitudes in Eq. (19) can have zero or nonzero values depending on the final state mesons. In the SM we see that  $\mathcal{A}_u^{\text{tree}} \gg \mathcal{A}_u^{\text{QCD}}, \mathcal{A}_u^{\text{EW}}, \mathcal{A}_c^{\text{non-cc}}$  due to

**Table 1**

Branching ratios in units  $10^{-6}$  of  $B \rightarrow \pi K^*$  and  $B \rightarrow \rho K$  decays. For comparison, we list the experimental results given in Ref. [1]. The first uncertainty in the predictions is due to the uncertainties in SCET parameters while the second uncertainty is due to the uncertainties in the CKM matrix elements.

Decay channel	Exp.	SM prediction
$\pi^0 K^{(*)+}$	$6.9 \pm 2.3$	$7.2^{+0.3+1.1}_{-0.2-0.9}$
$\pi^- K^{(*)+}$	$8.6 \pm 0.9$	$7.8^{+0.2+1.1}_{-0.2-1.0}$
$\pi^0 \bar{K}^{(*)0}$	$2.4 \pm 0.7$	$7.8^{+0.5+1.2}_{-0.5-1.0}$
$\pi^+ \bar{K}^{(*)0}$	$9.9^{+0.8}_{-0.9}$	$10.3^{+0.7+1.7}_{-0.7-1.4}$
$\rho^0 K^+$	$3.81^{+0.48}_{-0.46}$	$4.8^{+0.6+0.8}_{-0.6-0.7}$
$\rho^+ \bar{K}^0$	$8.0^{+1.5}_{-1.4}$	$10.9^{+0.6+1.7}_{-0.6-1.5}$
$\rho^0 \bar{K}^0$	$4.7 \pm 0.7$	$10.2^{+0.6+1.6}_{-0.6-1.4}$
$\rho^- K^+$	$8.6^{+0.9}_{-1.1}$	$2.6^{+0.5+0.4}_{-0.4-0.4}$

the hierarchy of the Wilson coefficients  $C_{1,2} \gg C_{3-10}$ . One should note that the amplitudes  $\mathcal{A}_u^{\text{QCD}}, \mathcal{A}_u^{EW}, \mathcal{A}_c^{\text{non-cc}}$  can receive contributions from QCD corrections that are proportional to the large Wilson coefficients  $C_{1,2,8g}$ .

The dominant NLO QCD corrections to Wilson coefficients given in Refs. [21,20,15,22,23,18] are taken into account in our analysis. These corrections are important since they contribute to the strong phase required for CP violation. In fact contributions to the strong phase from NLO QCD corrections to  $\mathcal{A}_u^{\text{tree}}, \mathcal{A}_u^{\text{QCD}}, \mathcal{A}_u^{EW}$  will be suppressed roughly speaking by a factor  $\alpha_s/\pi \times \frac{|\lambda_u^s|}{|\lambda_c^s|} \sim 0.0008$  in comparison with the strong phase of the charm penguin. On the other hand NLO QCD corrections to  $\mathcal{A}_c^{\text{non-cc}}$  will be suppressed roughly speaking by a factor  $\alpha_s/\pi \sim 0.04$  in comparison with the strong phase of the charm penguin. Thus, in SCET, the strong phase of the charm penguin is the dominant in all cases.

Now we consider two cases, first case we have  $\mathcal{A}_u^{\text{tree}} = 0$  while the second  $\mathcal{A}_u^{\text{tree}} \neq 0$ . In the first case we can write to a good approximation, after using  $\frac{|\lambda_u^s|}{|\lambda_c^s|} \sim 0.02$ ,

$$\mathcal{A} = \lambda_c^s (\mathcal{A}_c^{\text{cc}} + \mathcal{A}_c^{\text{non-cc}}) \quad (20)$$

which shows that the long distance charm penguin gives the dominant contribution to the amplitude as  $\mathcal{A}_c^{\text{non-cc}}$  are highly suppressed by the Wilson coefficients  $C_{3-10}$ . As an example for this case, the decay modes  $B^+ \rightarrow \pi^+ \bar{K}^{(*)0}$  and  $B^+ \rightarrow \rho^+ \bar{K}^0$  where  $\mathcal{A}_u^{\text{tree}} = 0$  and thus we expect that  $Br(B^+ \rightarrow \pi^+ \bar{K}^{(*)0}) \sim Br(B^+ \rightarrow \rho^+ \bar{K}^0)$  which is clear from Table 1.

Turning now to the second case where  $\mathcal{A}_u^{\text{tree}} \neq 0$ , to a good approximation we can write

$$\mathcal{A} = \lambda_u^s \mathcal{A}_u^{\text{tree}} + \lambda_c^s (\mathcal{A}_c^{\text{cc}} + \mathcal{A}_c^{\text{non-cc}}) \quad (21)$$

which shows also that the long distance charm penguin gives the dominant contribution to the amplitude, as  $\mathcal{A}_u^{\text{tree}}$  will be suppressed by a factor  $|\lambda_u^s| \sim 0.02 |\lambda_c^s|$  in comparison to  $\mathcal{A}_c^{\text{cc}}$ . Thus in all cases the long distance charm penguin gives the dominant contribution and as a consequence the amplitude in each decay mode will be of the same order of the long distance charming penguin amplitude.

For decay modes which do not receive contribution from charm penguin one expects very small branching ratios. Hence non-perturbative charming penguin plays crucial rule in the branching ratios using SCET.

The branching ratios of the decay modes  $B \rightarrow \pi K^*$  and  $B \rightarrow \rho K$  are given in Table 1 where the first uncertainty in the predictions is due to the uncertainties in SCET parameters while the second uncertainty is due to the uncertainties in the CKM matrix

**Table 2**

Direct CP asymmetries of  $B \rightarrow \pi K^*$  and  $B \rightarrow \rho K$  decays. As before, we list the experimental results given in Ref. [1]. The first uncertainty in the predictions is due to the uncertainties in SCET parameters while the second uncertainty is due to the uncertainties in the CKM matrix elements.

Decay channel	Exp.	SM prediction
$\pi^0 K^{*+}$	$0.04 \pm 0.29$	$-0.08^{+0.03+0.002}_{-0.03-0.002}$
$\pi^- K^{*+}$	$-0.18 \pm 0.07$	$-0.12^{+0.04+0.01}_{-0.03-0.001}$
$\pi^0 \bar{K}^{*0}$	$-0.15 \pm 0.12$	$-0.01^{+0.002+0.0003}_{-0.003-0.003}$
$\pi^+ \bar{K}^{*0}$	$-0.038 \pm 0.042$	$-0.004^{+0.001+0.001}_{-0.001-0.0003}$
$\rho^0 K^+$	$0.37 \pm 0.11$	$0.06^{+0.07+0.002}_{-0.08-0.002}$
$\rho^+ \bar{K}^0$	$-0.12 \pm 0.17$	$-0.005^{+0.001+0.0004}_{-0.001-0.0001}$
$\rho^0 \bar{K}^0$	$-0.02 \pm 0.27 \pm 0.08 \pm 0.06$	$-0.02^{+0.01+0.002}_{-0.01-0.001}$
$\rho^- K^+$	$0.15 \pm 0.06$	$0.14^{+0.11+0.004}_{-0.11-0.01}$

elements. As can be seen from that table, within SM, the branching ratios are in agreements with their corresponding experimental values in most of the decay modes.

Turning now to the SM predictions for the CP asymmetries which are presented in Table 2 where, as before, where the first uncertainty in the predictions is due to the uncertainties in SCET parameters while the second uncertainty is due to the uncertainties in the CKM matrix elements. Clearly from the table, the SM predictions for the CP asymmetries of  $B^+ \rightarrow \pi^0 K^{*+}$  has different sign in comparison with the experimental measurement and the predicted CP asymmetries in many of the decay modes are in agreement with the experimental measurements due to the large errors in these measurements. Moreover, we see from the table that, the predicted CP asymmetry of  $\bar{B} \rightarrow \pi^0 \bar{K}^{*0}$  and  $B^+ \rightarrow \rho^0 K^+$  disagree with the experimental results within  $1\sigma$  error of the experimental data. This can be attributed to the lack of the weak CP violating phases as SM Wilson coefficients are real and the only source of the weak phase is the phase of the CKM matrix.

Note, SCET provides large strong phases and thus with new sources of weak CP violation one would expect enhancement in these asymmetries. In the next section we consider the case of SUSY models with non-universal A terms where new sources of weak CP phases exist.

#### 4. SUSY contributions to the CP asymmetries of $B \rightarrow \rho K$ and $B \rightarrow \pi K^*$

In this section we analyze the SUSY contributions to the CP asymmetries of  $B^- \rightarrow \pi^- \bar{K}^{(*)0}$ ,  $B^- \rightarrow \rho^- \bar{K}^0$ ,  $\bar{B}^0 \rightarrow \rho^+ K^-$  and  $B^- \rightarrow \rho^0 K^-$  as their SM prediction is very small and cannot accommodate the experimental results. In SUSY, Flavor Changing Neutral Current (FCNC) and CP quantities are sensitive to particular entries in the mass matrices of the scalar fermions. Thus it is useful to adopt a model independent-parametrization, the so-called Mass Insertion Approximation (MIA) where all the couplings of fermions and sfermions to neutral gauginos are flavor diagonal [32]. Denoting by  $\Delta$  the off-diagonal terms in the  $(M_{\tilde{f}}^2)_{AB}$  where  $\tilde{f}$  denotes any scalar fermion and  $A, B$  indicate chirality,  $A, B = (L, R)$ :

$$(M_{\tilde{f}}^2)_{AB} = \begin{pmatrix} (m_{\tilde{f}1}^2)_{AB} & (\Delta_{AB}^f)_{12} & (\Delta_{AB}^f)_{13} \\ (\Delta_{AB}^f)_{21} & (m_{\tilde{f}2}^2)_{AB} & (\Delta_{AB}^f)_{23} \\ (\Delta_{AB}^f)_{31} & (\Delta_{AB}^f)_{32} & (m_{\tilde{f}3}^2)_{AB} \end{pmatrix}, \quad (22)$$

$\Delta_{LL}^{IJ} = \Delta_{LL}^{J I*}$  and  $\Delta_{RR}^{IJ} = \Delta_{RR}^{J I*}$ , but no such relation holds for  $\Delta_{LR}$ . It is often to set  $(m_{\tilde{f}1}^2)_{AB} = (m_{\tilde{f}2}^2)_{AB} = (m_{\tilde{f}3}^2)_{AB} = \tilde{m}^2$  where  $\tilde{m}$  is the

average sfermion mass. The Flavor Changing structure of the  $A - B$  sfermion propagator is exhibited by its non-diagonality and it can be expanded as

$$\begin{aligned} (\tilde{f}_A^a \tilde{f}_B^{b*}) &= i(k^2 I - \tilde{m}^2 I - \Delta_{AB}^f)^{-1} \\ &\simeq \frac{i\delta_{ab}}{k^2 - \tilde{m}^2} + \frac{i(\Delta_{AB}^f)_{ab}}{(k^2 - \tilde{m}^2)^2} + O(\Delta^2), \end{aligned} \quad (23)$$

where  $a, b = (1, 2, 3)$  are flavor indices and  $I$  is the unit matrix. It is convenient to define a dimensionless quantity  $(\delta_{AB}^f)_{ab} \equiv (\Delta_{AB}^f)_{ab}/\tilde{m}^2$ . As long as  $(\Delta_{AB}^f)_{ab}$  is smaller than  $\tilde{m}^2$  we can consider only the first order term in  $(\delta_{AB}^f)_{ab}$  of the sfermion propagator expansion.

The parameters  $(\delta_{AB}^f)_{ab}$  can be constrained through vacuum stability argument [33], experimental measurements concerning FCNC and CP violating phenomena [34]. Recent studies about other possible constraints can be found in Refs. [35–37].

At next leading order in  $\alpha_s$  expansion, the dominant SUSY contributions to our decay modes are originated from diagrams mediated by the exchange of gluino and chargino. The complete expressions for the gluino and chargino contributions to the Wilson coefficients can be found in Refs. [39,40,34,38].

After including SUSY contributions to the mentioned decays and keeping the dominant terms we find

$$\begin{aligned} A(B^- \rightarrow \pi^- \bar{K}^{(*)0}) &\times 10^7 \\ &\simeq -0.0178(\delta_{LL}^d)_{23} - 6.6914(\delta_{LR}^d)_{23} - 1.5857(\delta_{RL}^d)_{23} \\ &\quad - (0.0052 + 0.0003i)(\delta_{LR}^u)_{32} - (0.0046 - 0.0003i)(\delta_{RL}^u)_{32} \\ &\quad + (0.3319 - 0.0612i), \\ A(B^- \rightarrow \pi^0 \bar{K}^{(*)-}) &\times 10^7 \\ &\simeq 0.0125(\delta_{LL}^d)_{23} + 4.7315(\delta_{LR}^d)_{23} + 1.1212(\delta_{RL}^d)_{23} \\ &\quad + (0.0056 - 0.0001i)(\delta_{LR}^u)_{32} - (0.0223 - 0.0001i)(\delta_{RL}^u)_{32} \\ &\quad + (0.2508 - 0.1259i), \\ A(B^0 \rightarrow \pi^0 \bar{K}^{(*)0}) &\times 10^7 \\ &\simeq -0.0127(\delta_{LL}^d)_{23} - 4.7315(\delta_{LR}^d)_{23} - 1.1212(\delta_{RL}^d)_{23} \\ &\quad + (0.0094 + 0.0001i)(\delta_{LR}^u)_{32} - (0.0185 + 0.0001i)(\delta_{RL}^u)_{32} \\ &\quad + (0.2949 - 0.0707i), \\ A(B^0 \rightarrow \pi^+ \bar{K}^{(*)-}) &\times 10^7 \\ &\simeq 0.0178(\delta_{LL}^d)_{23} + 6.6914(\delta_{LR}^d)_{23} + 1.5857(\delta_{RL}^d)_{23} \\ &\quad - (0.0106 + 0.0005i)(\delta_{LR}^u)_{32} - (0.0099 - 0.0005i)(\delta_{RL}^u)_{32} \\ &\quad + (0.2695 - 0.1392i), \\ A(\bar{B}^- \rightarrow \rho^- K^0) &\times 10^7 \\ &\simeq 0.0043(\delta_{LL}^d)_{23} + 1.6190(\delta_{LR}^d)_{23} - 1.0851(\delta_{RL}^d)_{23} \\ &\quad - (0.0001 + 0.0005i)(\delta_{LR}^u)_{32} - (0.0021 - 0.0005i)(\delta_{RL}^u)_{32} \\ &\quad - (0.3473 + 0.0111i), \\ A(B^- \rightarrow \rho^0 K^-) &\times 10^7 \\ &\simeq -0.0031(\delta_{LL}^d)_{23} - 1.1448(\delta_{LR}^d)_{23} + 0.7673(\delta_{RL}^d)_{23} \\ &\quad - (0.0037 + 0.0006i)(\delta_{LR}^u)_{32} - (0.0120 - 0.0006i)(\delta_{RL}^u)_{32} \\ &\quad - (0.2232 + 0.0501i), \end{aligned}$$

$$\begin{aligned} A(\bar{B}^0 \rightarrow \rho^0 K^0) &\times 10^7 \\ &\simeq 0.0030(\delta_{LL}^d)_{23} + 1.1448(\delta_{LR}^d)_{23} - 0.7673(\delta_{RL}^d)_{23} \\ &\quad - (0.0032 + 0.0003i)(\delta_{LR}^u)_{32} - (0.0108 - 0.0003i)(\delta_{RL}^u)_{32} \\ &\quad - (0.3470 + 0.0307i), \\ A(B^- \rightarrow \rho^+ K^-) &\times 10^7 \\ &\simeq -0.0043(\delta_{LL}^d)_{23} - 1.6190(\delta_{LR}^d)_{23} + 1.0851(\delta_{RL}^d)_{23} \\ &\quad - (0.0008 + 0.0010i)(\delta_{LR}^u)_{32} - (0.0037 - 0.0010i)(\delta_{RL}^u)_{32} \\ &\quad - (0.1723 + 0.0386i). \end{aligned} \quad (24)$$

The mass insertions  $(\delta_{RL}^u)_{32}$  and  $(\delta_{LR}^u)_{32}$  are not constrained by  $b \rightarrow s\gamma$  and so we can set them as  $(\delta_{RL}^u)_{32} = (\delta_{LR}^u)_{32} = e^{i\delta_u}$  where  $\delta_u$  is the phase that can vary from  $-\pi$  to  $\pi$ . It should be noted that in order to have a well-defined Mass Insertion Approximation scheme, it is necessary to have

$|(\delta_{AB}^f)_{ab}| < 1$  but here in order to maximize the SUSY CP-violating contributions we take it of order one. Applying  $b \rightarrow s\gamma$  constraints leads to the following parametrization [41]

$$(\delta_{LL}^d)_{23} = e^{i\delta_d}, \quad (\delta_{LR}^d)_{23} = (\delta_{RL}^d)_{23} = 0.01e^{i\delta}. \quad (25)$$

In the following we present our results for the CP asymmetries. In our analysis we consider two scenarios, the first one with a single mass insertion where we keep only one mass insertion per time and take the other mass insertions to be zero and the second scenario with two mass insertions will be considered only in the cases when one single mass insertion is not sufficient to accommodate the experimental measurement. After setting the different mass insertions as mentioned above, we see from Eq. (24) that, the terms that contain the mass insertions  $(\delta_{RL}^u)_{32}$  and  $(\delta_{LR}^u)_{32}$  will be small in comparison with the other terms and thus we expect that their contributions to the asymmetries will be small. These terms are obtained from diagrams mediated by the chargino exchange and thus we see that gluino contributions give the dominant contributions as known in the literature.

We start our analysis of the direct CP asymmetries by considering the first scenario in which we take only one mass insertion corresponding to the gluino mediation and set the others to be zero.

After substituting the mass insertions given in Eq. (25), in Eq. (24) we find that the first and third terms in the amplitudes  $B^+ \rightarrow \pi^+ \bar{K}^{*0}$  and  $B^+ \rightarrow \pi^0 K^{*+}$  will be approximately equal and both of them will be smaller than the second term. As a consequence, one predicts that the asymmetries generated by the mass insertions  $(\delta_{LL}^d)_{23}$  and  $(\delta_{RL}^d)_{23}$  will be equal and in the same time these asymmetries will be smaller than the case of using  $(\delta_{LR}^d)_{23}$  which can be seen from Fig. 1. In that figure, we plot the CP asymmetries,  $A_{CP}(B^+ \rightarrow \pi^+ \bar{K}^{*0})$  and  $A_{CP}(B^+ \rightarrow \pi^0 K^{*+})$  versus the phase of the  $(\delta_{AB}^d)_{32}$  where  $A$  and  $B$  denote the chirality i.e.  $L$  and  $R$ , for 3 different mass insertions. The horizontal lines in both diagrams represent the experimental measurements to  $1\sigma$ . As can be seen from Fig. 1 left, for all gluino mass insertions, the value of the CP asymmetry  $A_{CP}(B^+ \rightarrow \pi^+ \bar{K}^{*0})$  is enhanced to accommodate the experimental measurement of the asymmetry within  $1\sigma$  for many values of the phase of the mass insertions. On the other hand, Fig. 1 right shows that the CP asymmetry  $A_{CP}(B^+ \rightarrow \pi^0 K^{*+})$  is enhanced to accommodate the experimental measurement within  $1\sigma$  for all values of the phase of the mass insertions. The point we stress here is that SUSY Wilson coefficients provide source of large weak phases, which are needed for accommodation of CP asymmetries.

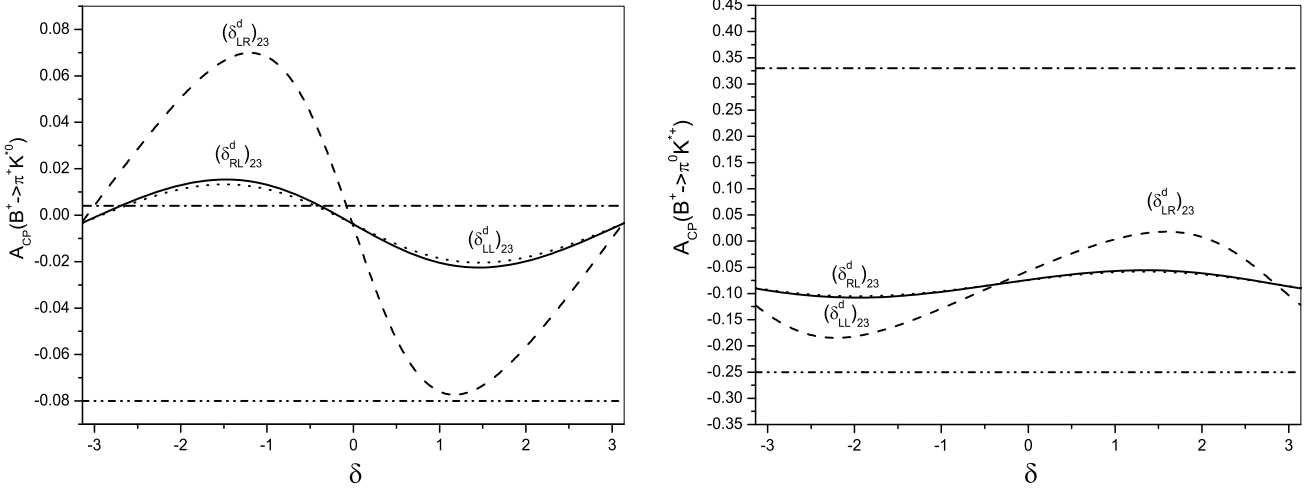


**Fig. 1.** CP asymmetries versus the phase of the  $(\delta_{AB}^d)_{23}$  where  $A$  and  $B$  denote the chirality i.e.  $L, R$ , for 3 different mass insertions. The left diagram corresponds to  $A_{CP}(B^+ \rightarrow \pi^+ K^0)$  while the right diagram corresponds to  $A_{CP}(B^+ \rightarrow \pi^0 K^+)$ . In both diagrams we take only one mass insertion per time and vary the phase of from  $-\pi$  to  $\pi$ . The horizontal lines in both diagrams represent the experimental measurement to  $1\sigma$ .

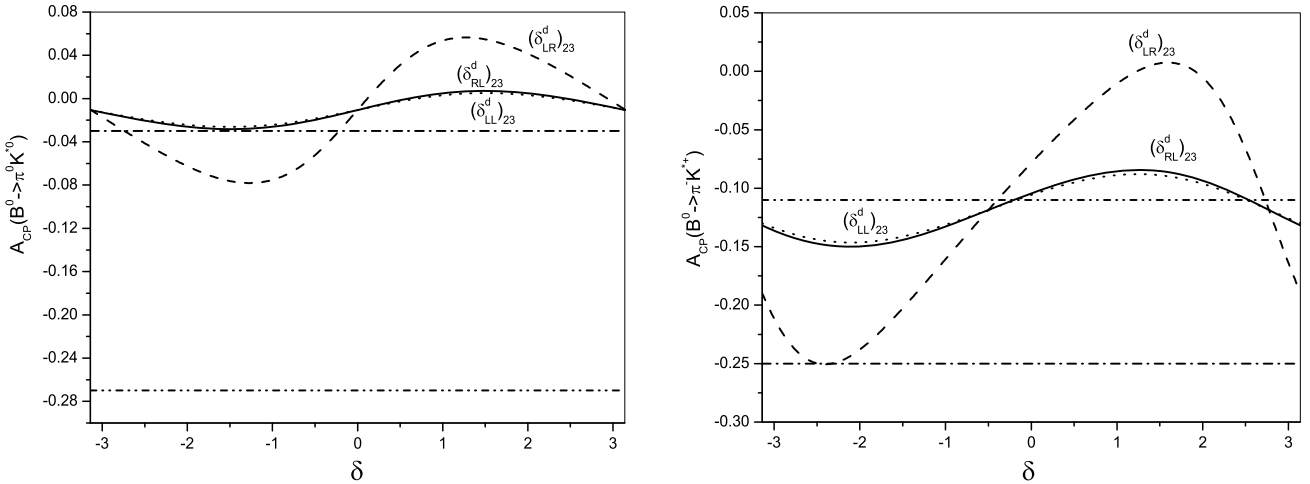


**Fig. 2.** CP asymmetries versus the phase of the  $(\delta_{AB}^d)_{23}$  where  $A$  and  $B$  denote the chirality i.e.  $L, R$ , for 3 different mass insertions. The left diagram corresponds to  $A_{CP}(B^0 \rightarrow \pi^0 \bar{K}^{*0})$  while the right diagram corresponds to  $A_{CP}(B^0 \rightarrow \pi^- K^{*+})$ . In both diagrams we take only one mass insertion per time and vary the phase of from  $-\pi$  to  $\pi$ . The horizontal lines in both diagrams represent the experimental measurement to  $1\sigma$ .

In Fig. 2 we plot the two asymmetries,  $A_{CP}(B^0 \rightarrow \pi^0 \bar{K}^{*0})$  and  $A_{CP}(B^0 \rightarrow \pi^- K^{*+})$  versus the phase of the  $(\delta_{AB}^d)_{32}$  as before. As can be seen from Fig. 2 left,  $A_{CP}(B^0 \rightarrow \pi^0 \bar{K}^{*0})$  lies within  $1\sigma$  range of its experimental value for many values of the phase of the mass insertion  $(\delta_{LR}^d)_{23}$  only. The reason for that is as before (see Eq. (24)), the two mass insertions  $(\delta_{LL}^d)_{23}$  and  $(\delta_{RL}^d)_{23}$  will give equal contributions to the CP asymmetries which will be smaller than the case of using  $(\delta_{LR}^d)_{23}$ . On the other hand, Fig. 2 right, we see that  $A_{CP}(B^0 \rightarrow \pi^- K^{*+})$  can be accommodated within  $1\sigma$  for many values of the phase of the three gluino mass insertions.

Finally we discuss the CP asymmetries of the decay modes  $B^+ \rightarrow \rho^+ K^0$  and  $B^+ \rightarrow \rho^0 K^+$ . After substituting the mass insertions given in Eq. (25) in Eq. (24), we find that the first and third terms in the amplitudes  $B^+ \rightarrow \rho^+ K^0$  and  $B^+ \rightarrow \rho^0 K^+$  will be no longer equal as previous cases and thus we expect their contributions to the asymmetries will be different which can be seen from Fig. 3 where, as before, we plot  $A_{CP}(B^+ \rightarrow \rho^+ K^0)$  and  $A_{CP}(B^+ \rightarrow \rho^0 K^+)$  versus the phase of the  $(\delta_{AB}^d)_{23}$ . In Fig. 3 we do not show the horizontal lines representing the  $1\sigma$  range of the experimental

measurement as the three curves of the  $A_{CP}(B^+ \rightarrow \rho^+ K^0)$  corresponding to the three gluino mass insertions totally lie in this  $1\sigma$  range for all values of the phase of the mass insertions. On the other hand, Fig. 3 right, we see that  $A_{CP}(B^+ \rightarrow \rho^0 K^+)$  cannot be accommodated within  $1\sigma$  for any value of the phase of all gluino mass insertions. This motivates us to consider the second scenario with two mass insertions.

In Fig. 4, we plot the CP asymmetry,  $A_{CP}(B^+ \rightarrow \rho^0 K^+)$  versus the phase of the mass insertion for 2 different mass insertions. The left diagram correspond to gluino contributions where we keep the two mass insertions  $(\delta_{LR}^d)_{23}$  and  $(\delta_{RL}^d)_{23}$  and set the other mass insertions to zero. The right diagram correspond to both gluino and chargino contributions where we keep the two mass insertions  $(\delta_{LR}^d)_{23}$  and  $(\delta_{RL}^d)_{32}$  and set the other mass insertions to zero. In both diagrams we assume that the two mass insertion have equal phases and we vary the phase from  $-\pi$  to  $\pi$ . As before, the horizontal lines in both diagrams represent the experimental measurement to  $1\sigma$ . As can be seen from Fig. 4 left, two gluino mass insertions cannot accommodate the experimental measurement for any value of the phase of the mass insertion.

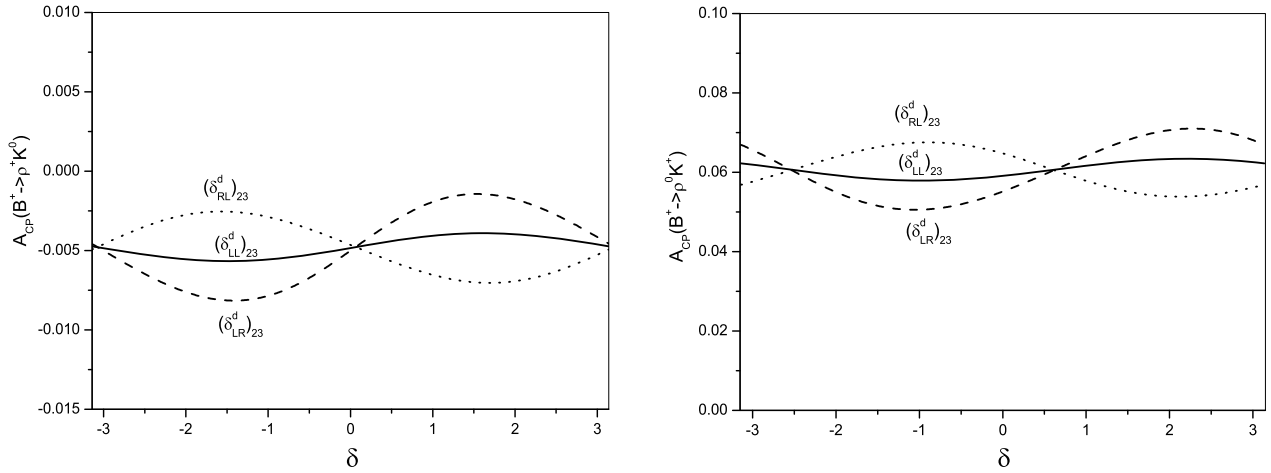


**Fig. 3.** CP asymmetries versus the phase of the  $(\delta^d_{AB})_{23}$  where  $A$  and  $B$  denote the chirality i.e.  $L, R$ , for 3 different mass insertions. The left diagram corresponds to  $A_{CP}(B^+ \rightarrow \rho^+ K^0)$  while the right diagram corresponds to  $A_{CP}(B^+ \rightarrow \rho^0 K^+)$ . In both diagrams we take only one mass insertion per time and vary the phase of from  $-\pi$  to  $\pi$ .

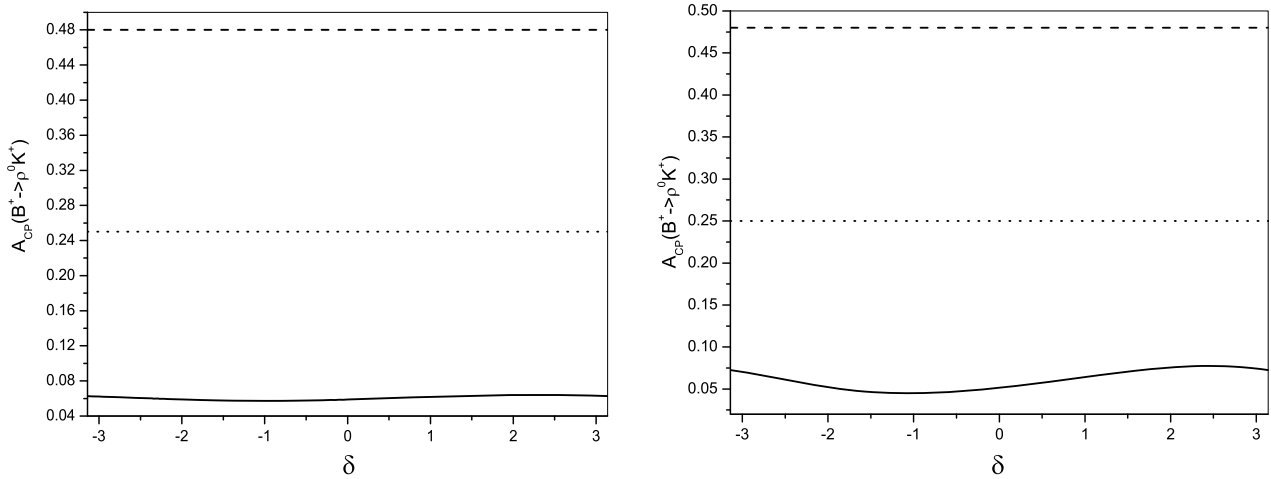


**Fig. 4.** CP asymmetry of  $A_{CP}(B^+ \rightarrow \rho^0 K^+)$  versus the phase of the mass insertion for 2 different mass insertions. The left diagram correspond to gluino contributions where we keep the two mass insertions  $(\delta^d_{LR})_{23}$  and  $(\delta^d_{RL})_{23}$  and set the other mass insertions to zero. The right diagram correspond to both gluino and chargino contributions where we keep the two mass insertions  $(\delta^d_{LR})_{23}$  and  $(\delta^u_{RL})_{32}$  and set the other mass insertions to zero. In both diagrams we assume that the two mass insertion have equal phases and we vary the phase from  $-\pi$  to  $\pi$ . The horizontal lines in both diagrams represent the experimental measurements to  $1\sigma$ .

On the other hand from Fig. 4 right, two mass insertions one corresponding to chargino contribution and the other corresponding to gluino contribution cannot accommodate the experimental measurements. We find that in order to accommodate the CP symmetry in this case the Wilson coefficient  $C_9^{glu}$  should be increased at least by a factor  $-6\pi/\alpha$  without violating any constraints on the SUSY parameter space. We show the corresponding diagram in Fig. 5.

**5. Conclusion**

Within Soft Collinear Effective Theory, we extend the Standard Model analysis of the  $B \rightarrow \pi K^*$  and  $B \rightarrow \rho K$  asymmetries to include the next leading order QCD corrections. We find that, even with QCD correction, the Standard Model predictions cannot accommodate the direct CP asymmetries in these decay modes.

We have analyzed the SUSY contributions to the direct CP asymmetries of the decay modes  $B \rightarrow \rho K$  and  $B \rightarrow \pi K^*$  using the Mass Insertion Approximation. Contrarily to SM, our results show that these direct CP asymmetries can be significantly enhanced by the SUSY contributions mediated by gluino exchange and thus accommodate the experimental results.

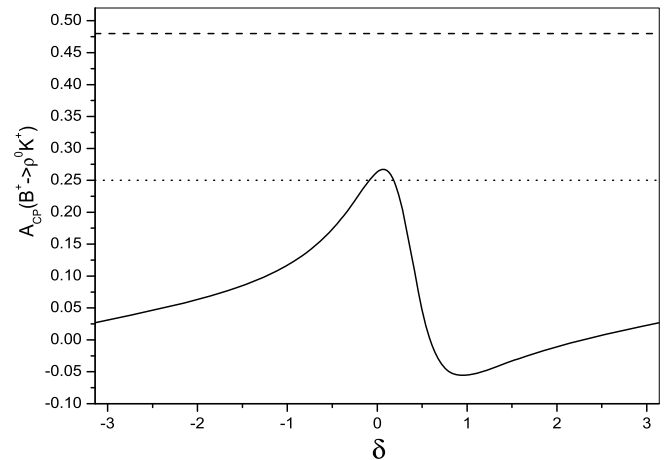


**Fig. 5.** CP asymmetry of  $A_{CP}(B^+ \rightarrow \rho^0 K^+)$  versus the phase of the mass insertion for 2 different mass insertions correspond to gluino contributions where we keep the two mass insertions  $(\delta^d_{LR})_{23}$  and  $(\delta^d_{RL})_{23}$  and set the other mass insertions to zero. We assume that the two mass insertion have equal phases and we vary the phase from  $-\pi$  to  $\pi$ . The horizontal lines in the diagram represent the experimental measurements to  $1\sigma$ .

## Acknowledgements

Gaber Faisel's work is supported by the National Science Council of R.O.C. under grants NSC 99-2112-M-008-003-MY3 and NSC 99-2811-M-008-085. D.D. has been supported by PROMEP and DINPO project from Guanajuato University.

## References

- [1] The Heavy Flavor Averaging Group, arXiv:1010.1589 [hep-ex].
- [2] M. Beneke, M. Neubert, Nucl. Phys. B 675 (2003) 333, arXiv:hep-ph/0308039.
- [3] C.D. Lu, M.Z. Yang, Eur. Phys. J. C 23 (2002) 275, arXiv:hep-ph/0011238.
- [4] X. Liu, H.s. Wang, Z.j. Xiao, L. Guo, C.D. Lu, Phys. Rev. D 73 (2006) 074002, arXiv:hep-ph/0509362.
- [5] D.Q. Guo, X.F. Chen, Z.J. Xiao, Phys. Rev. D 75 (2007) 054033, arXiv:hep-ph/0702110.
- [6] L. Guo, Q.g. Xu, Z.j. Xiao, Phys. Rev. D 75 (2007) 014019, arXiv:hep-ph/0609005.
- [7] W. Wang, Y.M. Wang, D.S. Yang, C.D. Lu, Phys. Rev. D 78 (2008) 034011, arXiv:0801.3123 [hep-ph].
- [8] C.W. Chiang, D. London, Mod. Phys. Lett. A 24 (2009) 1983, arXiv:0904.2235 [hep-ph].
- [9] D. Delepine, G. Faisel, S. Khalil, M. Shalaby, Int. J. Mod. Phys. A 22 (2007) 6011.
- [10] D. Delepine, G. Faisel, S. Khalil, Phys. Rev. D 77 (2008) 016003, arXiv:0710.1441 [hep-ph].
- [11] D. Delepine, G. Faisl, S. Khalil, G.L. Castro, Phys. Rev. D 74 (2006) 056004, arXiv:hep-ph/0608008.
- [12] C.W. Bauer, S. Fleming, M.E. Luke, Phys. Rev. D 63 (2000) 014006, arXiv:hep-ph/0005275.
- [13] C.W. Bauer, S. Fleming, D. Pirjol, I.W. Stewart, Phys. Rev. D 63 (2001) 114020, arXiv:hep-ph/0011336.
- [14] J. Chay, C. Kim, Phys. Rev. D 68 (2003) 071502, arXiv:hep-ph/0301055.
- [15] J. Chay, C. Kim, Nucl. Phys. B 680 (2004) 302, arXiv:hep-ph/0301262.
- [16] S. Fleming, PoS E FT09 (2009) 002, arXiv:0907.3897 [hep-ph].
- [17] C.W. Bauer, D. Pirjol, I.W. Stewart, Phys. Rev. D 67 (2003) 071502, arXiv:hep-ph/0211069.
- [18] A. Jain, I.Z. Rothstein, I.W. Stewart, arXiv:0706.3399 [hep-ph].
- [19] C.W. Bauer, D. Pirjol, I.Z. Rothstein, I.W. Stewart, Phys. Rev. D 70 (2004) 054015, arXiv:hep-ph/0401188.
- [20] M. Beneke, G. Buchalla, M. Neubert, C.T. Sachrajda, Nucl. Phys. B 591 (2000) 313, arXiv:hep-ph/0006124.
- [21] M. Beneke, G. Buchalla, M. Neubert, C.T. Sachrajda, Phys. Rev. Lett. 83 (1999) 1914, arXiv:hep-ph/9905312.
- [22] M. Beneke, S. Jager, Nucl. Phys. B 751 (2006) 160, arXiv:hep-ph/0512351.
- [23] M. Beneke, S. Jager, Nucl. Phys. B 768 (2007) 51, arXiv:hep-ph/0610322.
- [24] C.M. Arnesen, Z. Ligeti, I.Z. Rothstein, I.W. Stewart, arXiv:hep-ph/0607001.
- [25] A. Hardmeier, E. Lunghi, D. Pirjol, D. Wyler, Nucl. Phys. B 682 (2004) 150, arXiv:hep-ph/0307171.
- [26] Y.Y. Keum, H.n. Li, A.I. Sanda, Phys. Lett. B 504 (2001) 6, arXiv:hep-ph/0004004.
- [27] C.D. Lu, K. Ukai, M.Z. Yang, Phys. Rev. D 63 (2001) 074009, arXiv:hep-ph/0004213.
- [28] M. Beneke, G. Buchalla, M. Neubert, C.T. Sachrajda, Nucl. Phys. B 606 (2001) 245, arXiv:hep-ph/0104110.
- [29] A.L. Kagan, Phys. Lett. B 601 (2004) 151, arXiv:hep-ph/0405134.
- [30] A.V. Manohar, I.W. Stewart, Phys. Rev. D 76 (2007) 074002, arXiv:hep-ph/0605001.
- [31] G. Buchalla, A.J. Buras, M.E. Lautenbacher, Rev. Mod. Phys. 68 (1996) 1230, arXiv:hep-ph/9512380.
- [32] L.J. Hall, V.A. Kostelecky, S. Raby, Nucl. Phys. B 267 (1986) 415.
- [33] J.A. Casas, S. Dimopoulos, Phys. Lett. B 387 (1996) 107, arXiv:hep-ph/9606237.
- [34] F. Gabbiani, E. Gabrielli, A. Masiero, L. Silvestrini, Nucl. Phys. B 477 (1996) 321, arXiv:hep-ph/9604387.
- [35] A. Crivellin, U. Nierste, Phys. Rev. D 79 (2009) 035018, arXiv:0810.1613 [hep-ph].
- [36] A. Crivellin, U. Nierste, Phys. Rev. D 81 (2010) 095007, arXiv:0908.4404 [hep-ph].
- [37] A. Crivellin, J. Girrbach, Phys. Rev. D 81 (2010) 076001, arXiv:1002.0227 [hep-ph].
- [38] A.J. Buras, P. Gambino, M. Gorbahn, S. Jager, L. Silvestrini, Nucl. Phys. B 592 (2001) 55, arXiv:hep-ph/0007313.
- [39] S. Bertolini, F. Borzumati, A. Masiero, G. Ridolfi, Nucl. Phys. B 353 (1991) 591.
- [40] E. Gabrielli, G.F. Giudice, Nucl. Phys. B 433 (1995) 3, Nucl. Phys. B 507 (1997) 549 (Erratum), arXiv:hep-lat/9407029.
- [41] K. Huitu, S. Khalil, Phys. Rev. D 81 (2010) 095008, arXiv:0911.1868 [hep-ph].